IJBSCHS
[Original Article]

Biomedical Soft Computing and Human Sciences, Vol.20, No.1, pp.7-19

**(Accepted on 2015.3.9)**

# Effect of 1/6 Gravity Environment on Atmospheric Suspension of Simulated Lunar Regolith

Syou MAKI [1] *, Yoshiyuki HONMA [2], Hidetoshi TSUCHIYA [2], Kazunari TANAKA [2], Shigeru AOKI [2], Hajime TAKEOKA [2], Takeo MIKI [2], Hiroshi OHSHIMA [2], Masafumi YAMAMOTO [2], Yasuo MORIMOTO [3], Yasutaka OGAWA [1] and Chiaki MUKAI [2]

*1) Department of Hazard Evaluation and Epidemiology Research Group, National Institute of Occupational Safety and Health, Japan*

*2) Space Biomedical Research Office, Japan Aerospace Exploration Agency (JAXA)*

*3) Department of Occupational Pneumology, University of Occupational and Environmental Health, Japan*

***Abstract:*** *In order to investigate the behavior of suspended particle matter (SPM) in a 1/6 gravity (1/6 G) environment, simulated lunar regolith was diffused in a chamber, realizing a quasi 1/6 gravity environment by parabolic flight. The effect of the 1/6 G environment on the atmospheric suspension was evaluated by means of the cutoff value of an elutriator; the cutoff value in the 1/6 G should be* $\sqrt{6}$ *times larger than at the earth's surface. The results of our experiment confirmed that the falling velocity of SPM in a 1/6G approximates Stokes' law, and the falling time is inversely proportional to the force of gravity. Numerical computation suggested that residual SPM in a convection-free room becomes high in a low-gravity environment or in a high-ceilinged room. These results suggest that once lunar dust intruded into a lunar base, it would take a considerably long time to clean up. Since the suspension time of SPM is different according to the particle size, the exposure risk of SPM will also vary according to the particle size. Considering that the risk depends only on the drifting time, the actual influence of low gravity on fine particles (*$D_p \leq 1.0$ *mm in diameter) and on large particles (*$D_p > 10$ *mm) in a 1/6G would be negligible. In contrast, for medium sized particles (*$2.5 < D_p \leq 10$ *mm) the difference in the drifting time between that on the earth and on the lunar surface is much larger than can be confirmed with the senses. Safety precautions used for this size of particle on the earth should be altered on the lunar surface.*

***Keywords:*** SPM, elutriator, Stokes' law, regolith, dust proof

## 1. Introduction

According to the latest research, the surface of the moon is covered by a desolate and thick layer of dust [1-4]. The diameters of particles picked up from the moon surface range widely, from the order of nanometers to microns, and a variety of shapes can be observed. Among these particles (lunar regolith, hereafter), many matters with acicular shapes like asbestos have been discovered. Although details about the toxicity of lunar regolith are still unknown, moon dust is considered to be toxic because it has been exposed to solar rays for a long time[5]. The National Aeronautics and Space Administration (NASA) is also greatly interested in the toxicity of lunar regolith [6-8], and there is anxiety about serious effects on the health of human beings constructing living spaces in the atmosphere of the lunar surface in the future.

In an atmosphere where no convection or airflow is present, the settling and diffusion of suspended particle matter (SPM) are theoretically formulated by the particle size, viscous resistance of air, and gravity. On the surface of the moon, where gravity is about 1/6 that on the earth, SPM stays suspended much longer than on the earth. If there should be any ingress of lunar regolith into an

* present affiliation : Faculty of Pharmacy,
Osaka Ohtani University
3-11-1, Nishikiori-kita,Tondabayashi City,
Osaka Pref. 584-8540, Japan
Phone: +81-721-24-9468, Fax: +81-721-24-9890,
E-mail: makisyo@osaka-ohtani.ac.jp

enclosed living space, it would be suspended for a longer time than on the earth, and the state of dangerous contamination would continue longer. On the other hand, any airborne SPM would finally settle down on the floor, since regolith is not completely free from gravity. Once such particles settled down, they could not be removed with a dustproof device. Decontamination work would require a far longer time than that under no gravity.

As mentioned above, the ingress of even a small amount of lunar regolith would threaten the safety and health of astronauts, and, in addition, it could cause disruptions in the working environment. Some scientists are of the opinion that such ingress of moon dust into residential blocks would not actually occur because living spaces on the lunar surface will be fully equipped with air filters and dustproof equipment. On the other hand, when constructing a base on the the surface of the moon, it will be necessary to install the living facilities more than 9 meters under the ground in order to avoid radiation from the sun[9]. This fact is not well known. Although sufficient consideration is needed in regard to the dangers of lunar regolith, the problem of exposure to lunar regolith in the air phase in a gravity-reduced environment (i.e., partial gravity environment) has not been investigated yet, except for the studies by Miki et. al.[10, 11] In fact, even the presence of an exposure risk to fine particle matter in a partial gravity environment has not been recognized so much [12-15].

Therefore, we have investigated the behavior of SPM in the air phase in a field of 1/6 gravity (1/6G hereafter). We created an artificial environment of 1/6G in which simulated lunar regolith (simulant hereafter) was actually diffused so that we could observe the time-serial variations of the respective particles and quantities. Since there is no precedent research in regard to the effect of lunar gravitational force on the behavior of SPM, we referred to the relevant JIS Standard[16] and others relating to the settling of particles in a liquid phase in order to obtain our empirical results [17], and examined the effect of moon dust on health, based on this knowledge.

## 2. Method of Measurement

A well-known method to realize a partial gravity environment on the earth is the utilization of magnetic force or parabolic flight [18]. Although the use of magnetic force provides the advantage of maintaining a partial gravity environment for a long time, the available space in the field of a superconducting magnet is too small, and the effect of the radial component of the magnetic force cannot be neglected[19,20], making this method unsuitable for our intended experiment. For this reason, we adopted the empirical programs of parabolic flight.

Parabolic flight can produce approximately 30 seconds of a 1/6G environment, the same condition as is available on the the surface of the moon. We had to measure the number of particles and particle sizes during such a short duration of time. Consequently, we developed our new, unique empirical equipment that employs an "*elutriator*".

### *Equipment*

The elutriator is a device for classifying particles of a greater than specified size. A schematic illustration is shown in Fig.1. Inside the elutriator are installed horizontal multi-tier blades positioned at equal intervals. While the SPM passes through the blades, larger sized particles settle on the blades while smaller sized particles pass through the elutriator. The elutriator is generally equipped with a dust-collecting filter between (A) and (B) in Fig.1. During this experiment, however, we left this filer dislodged. The maximum size of a particle that can pass through the elutriator is called *the cutoff value*. The cutoff value has a close relationship with particle retention time and settling speed.

Fig. 2 is a schematic representation of the equipment. For our experiment we used a high-performance particle size measuring unit by the name of the APS (Aero dynamic

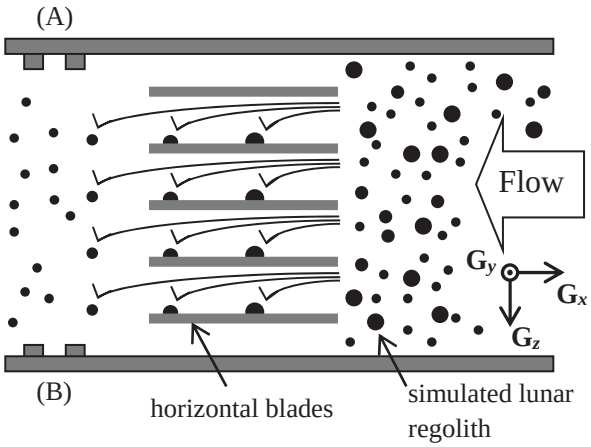


Fig.1 Schematic illustration of the elutriator. Basically, the elutriator is classifier equipment for large particles. Large particles cannot pass through and stay in stacks on the horizontal blades, and only small particles can pass through. Therefore, the filter primarily set at (A)-(B) was removed for this experiment.

Particle Sizer, Model 3321, TSI Co., Ltd.). The APS ((A) in Fig. 2) incorporates a suction pump with a capacity of 5 liters per minute. Particles drawn in together with air are processed at a 50-channel resolution, and a distribution diagram of particle sizes [μm] and the number of particles [count/cm$^3$] is produced every one second. The elutriator (C30, Sibata Co., Ltd.) ((B) in Fig. 2) is installed between the APS and the cylindrical chamber ((C) in Fig. 2). The flow rate of APS is designed not to influence the accuracy of elutriator.

Beneath the chamber is installed a blow-up device that is intended to diffuse the simulant into the atmosphere internally. Since the simulant that is blown up is drawn in by the suction pump together with air, the concentration of particles in the chamber continues to lower with time. To reduce the effect of the reduction of concentration to a minimum, the chamber size was determined to the maximum limitation permissible for parabolic flight. The chamber diameter and height are 259 mm and 425 mm, respectively. The chamber volume is 22.4 liters.

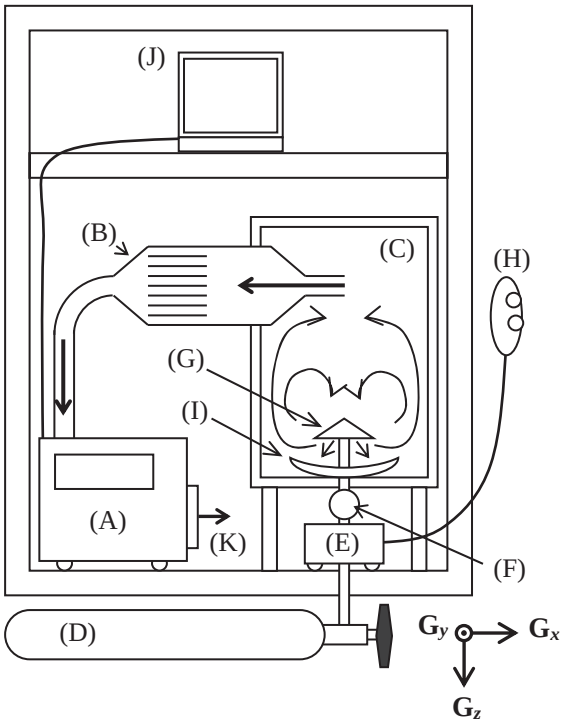


Fig.2 Scheme of the equipments. (A) Particle size measuring unit APS (Aerodynamic Particle Sizer, Model 3321, TSI Co., Ltd.), (B) elutriator without a dust-collecting filter, (C) cylindrical chamber, (D) compressed air cylinder, (E) reservoir tank, (F) simulant filling port, (G) nozzle, (H) remote control switch for solenoid valve, (I) cup-shaped reflector plate intended to diffuse the simulant into air, (J) personal computer for data recording, (K) HEPA filter (high-efficiency particle air filter) are installed in the APS. HEPA filters are also mounted on the top and the bottom of the chamber.

Practically, compressed air is used to blow up the simulant. Compressed air at 9.8 MPa ((D) in Fig. 2) is reduced as low as 0.15 MPa with a regulator and then temporarily kept in a reservoir tank ((E) in Fig. 2). In the blow-up process, the valve of the reservoir tank is tentatively opened so that the simulant set at the filling port ((F) in Fig. 2) of the tank located downstream can be pushed towards the chamber by the effect of compressed air flow. The simulant is discharged into the chamber from the nozzle of (G) in Fig. 2. The open-shut action of the valve is controlled by a solenoid valve. The timing for opening the valve is managed with a remote control switch ((H) in Fig. 2), and the duration of opening was set at 1.5 seconds. The simulant and compressed air discharged from the nozzle first collide with a cup-shaped reflector plate ((I) in Fig. 2) and are then diffused into the chamber inside. This nozzle and the reflector plate are the parts used for combustion testing as stipulated by the JIS Standard [21]. They are designed so that air and burning material can be uniformly mixed, allowing the simulant to diffuse into the chamber as uniformly as possible. The diffused simulant gets on the airflow of the pump and is led to the APS. The results of measurements are automatically recorded by a personal computer ((J) in Fig.2) connected externally.

The simulant and airflow are finally carried as far as the HEPA filter (high-efficiency particle air filter) installed in the APS, where the simulant is removed and air is discharged to the outside of the APS ((K) in Fig.2). HEPA filters are also mounted on the top and the bottom of the chamber in order to maintain constant pressure in the internal chamber.

For the purpose of reducing the effect of static electricity, the elutriator, chamber, nozzle, cup-shaped reflector plate, and other components are made of metallic materials. For the same reason, the chamber and the APS are connected through a conductive tube with an inner diameter of 20 mm and a length of 0.25 m. The time lag between opening the valve and measurement of the first simulant at the APS is approximately 3 seconds.

Horizontality is an essential factor for the measurement of cutoff values with the use of an elutriator. Therefore, the inclination of the equipment and the cutoff values were verified through ground testing. Results verified that the influence on the cutoff values is negligibly small so long as the inclination angle of the elutriator is kept within 10 degrees. Details are indicated in the Appendix.

Table 1. Comparison of chemical compositions of lunar dust and typical simulated lunar dust particles (simulant).

| | (1) | (2) | (3) |
|---|---|---|---|
| $SiO_2$ | 46.30 % | 45.00 | 49.14 |
| $TiO_2$ | 3.00 | 0.54 | 1.91 |
| $Al_2O_3$ | 12.90 | 27.30 | 16.23 |
| FeO | 15.10 | 5.10 | *13.07 |
| MnO | 0.22 | 0.30 | 0.19 |
| MgO | 9.30 | 5.70 | 3.84 |
| CaO | 10.70 | 15.70 | 9.13 |
| $Na_2O$ | 0.54 | 0.46 | 2.75 |
| Density [$g/cm^3$] | 2.5-3.2 | | 2.96 |

(1) Apollo-12, (2) Apollo-16, (3) FJS-1 by Shimizu Corp. (1) and (2) are the real lunar dust, and (3) is the simulated lunar dust (simulant) we used. All of these data were measured by NASA.
* amount of FeO and $Fe_2O_3$

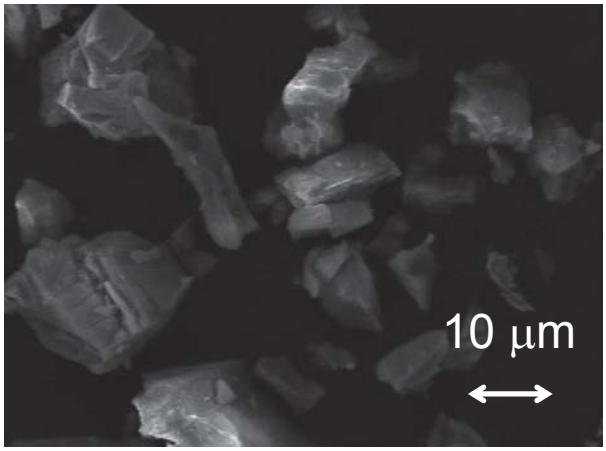


Fig.3 SEM Image (JIB-4500, JEOL Co., Ltd.) of simulated lunar dust particles FJS-1 (Shimizu Corp.). The raw material of FJS-1 is made from volcanic rock obtainable on the earth. Components of this material are almost the same as those of lunar regolith. Chemical components are shown in Table 1.

### *Simulated Lunar Regolith*

The simulated lunar regolith used in our research is FJS-1 manufactured by the Shimizu Corporation and is made from volcanic rock obtainable on the earth. The components of this material are almost the same as those of the lunar regolith sampled in the “Sea of Tranquility” on the moon. The chemical components are shown in Table 1. For our experiment, we used a sieve to adjust the dust size so that the particles could be kept within 20 μm. Fig. 3 shows FJS-1 photographed by a scanning electron micrograph (SEM). According to the previous research, FJS-1 was proven to be a ferromagnetic substance [22]. Other physical properties (optical, chemical, and magnetic) of actual lunar regolith were examined by Hapke et. al. [23]

## 3. Experiments

### *Setting the Cutoff Value*

In this experiment, the total number of particles was normalized based on the number of the largest particles measured. When the rate of particle count was less than 0.3%, it was regarded as a measurement error. When the number of present particles was 0.3% or more, the cutoff value was defined as the maximum simulant particle size measureable by the APS.

### *Quantity of Blowing Up*

Since the limit of particle measurement specified for the APS was 2000 particles per second, the simulant used for each blowing up was set at 0.035 to 0.045 g. The number of particles blown up in this experiment was 1452 to 1768 particles per second. Since this quantity was extremely small, it was absolutely impossible to observe any floating simulant with the naked eye shortly after blowing up.

The duration of compressed air flowing into the chamber at the time of blowing up was just 1.5 seconds, controlled accurately by the solenoid valve. Since the main body of the chamber was equipped with HEPA filters, there was almost no influence of internal pressure variations in the chamber on the diffusion of the SPM.

### *Timing of Blowing Up the Simulant*

The timing of blowing up the simulant is an important key to the results of the experiments. If the timing for blowing up is too early, most of the large particles fall down before the condition of 1/6G is assumed, and the estimated cutoff value is smaller. If the blowing up is delayed, on the contrary, the initial velocity remains in the floating particles and the state of floating SPM cannot be reproduced.

In consideration of the aforementioned points, we repeated the ground testing, coming to the conclusion that blowing up should start about 60 seconds before the

attainment of the state of the 1/6G condition. In other words, this timing is about 30 seconds before an airplane begins to perform parabolic flight.

The start-up time for data collection was set at 5 to 7 seconds before the start of blowing up. Since the data were continually collected at intervals of one second for 140 seconds, the data of particles classified in 140 particle sizes were time-serially collected during a single flight.

### *Parabolic Flight for 1/6G*

We flew on an off-centered course from a conventional parabolic locus in order to realize a 1/6G environment for approximately 30 seconds. In parabolic flight, however, a temporary hypergravity condition inside the cabin is inevitable before the aircraft goes into the environment of 1/6G. The first hypergravity condition is created while the aircraft follows a zooming process along a parabolic orbit. At that time, a hypergravity condition of approximately 1.8G continues for about 30 seconds. The state of 1/6G is realized shortly after the aircraft begins to descend sharply from the zenith of the parabolic line. After that, a second hypergravity condition is created in the process of horizontal flight after the aircraft raises its nose. In that case, the state of hypergravity is milder than that in the first case, and a condition of 1.5G to 1.6G continues for about 30 seconds. When horizontal flight is stabilized, the gravity in the cabin returns to 1G.

As described above, the gravity changes 4 times during data collection. Accordingly, in addition to the time-serial data collection in the state of 1/6G, we successfully collected time-serial data in the states of 1.8G and 1.5G. In this report, however, only the data of 1G and 1/6G have been used for analysis.

## 4. Results

Parabolic flights for 1/6G were carried out twice and experimental data were collected in both cases. The recorded pressure and temperature in the cabin were 0.082 ± 0.001 MPa and 20.5 ± 0.7°C, respectively.

In this report, the experiment (gravity 1G) performed in the aircraft during stable flight is called case A. The experiments performed twice at 1/6G during parabolic flight are called case B and case C. Variations in gravity measured in the aircraft for cases A - C are shown in Fig. 4. Typical data of the distribution of particles classified by particle size collected at that time are shown in Fig.5.

### *Gravity Variations in the cabin*

Gravity in the cabin was three-dimensionally measured at intervals of 0.5 seconds from shortly before taking off until landing. We defined as the direction of aircraft navigation is $G_x$, the right or left direction against the flying direction $G_y$, and the downward perpendicular direction against the flying direction $G_z$.

Figs. 4 (A) to (C) indicate the cahge of gravity in the

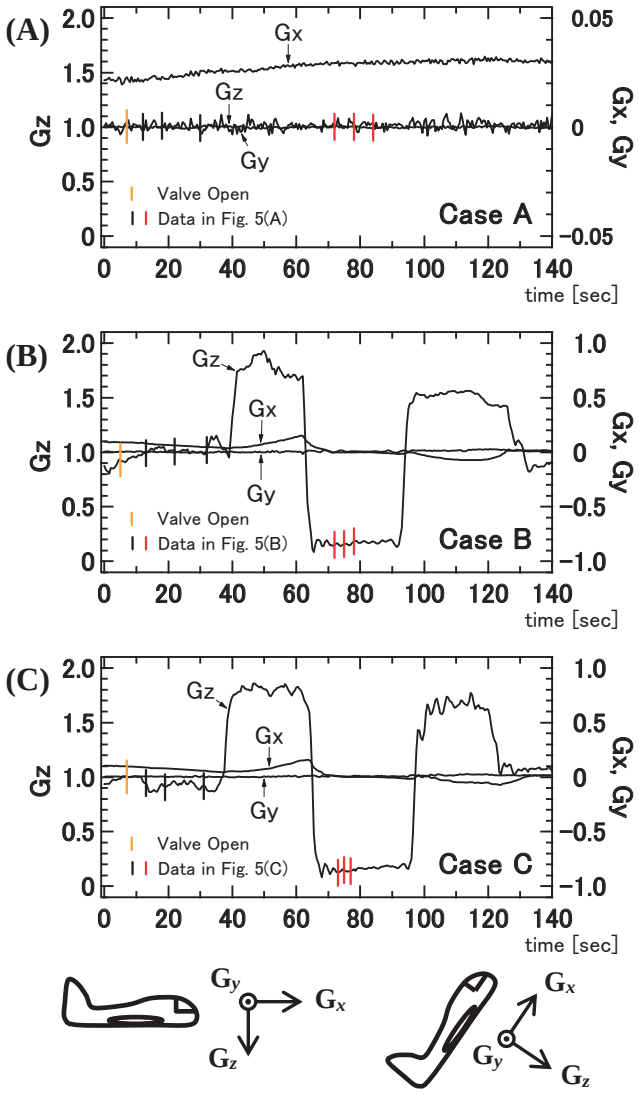


Fig.4 Variations in the gravity in the aircraft measured during parabolic flight. The left axis of ordinates shows the gravity component $G_z$ perpendicular to the aircraft. The right axis of ordinates shows the gravity component $G_x$ in aircraft forward direction and the gravity component $G_y$ in horizontal direction. The axis of abscissas shows time (in seconds). The solid yellow line shows the simulant blow-up time. Black (1G) and red (1/6G) bars show typical data measuring time, corresponding respectively to each gravity state in Fig. 5.

cabin. The "1.0 G" in Fig. 4 means the gravitational force on the earth. The magnitude of 0.17 corresponds to the state of 1/6 gravity. Diagrams (A) to (C) in Fig. 4 correspond to case A to case C, respectively. In $G_x$, some variations were observed at the time of the parabolic flight, but there were almost no variations in the state of 1/6G. In $G_y$, almost no variations were observed during the whole parabolic flight. In $G_z$, slight variations were seen during horizontal flight, but preferable stability was observed during the time (for 60 to 90 seconds after blowing up) when the state of 1/6G was maintained.

In Fig. 4, the time for blowing up is indicated by a

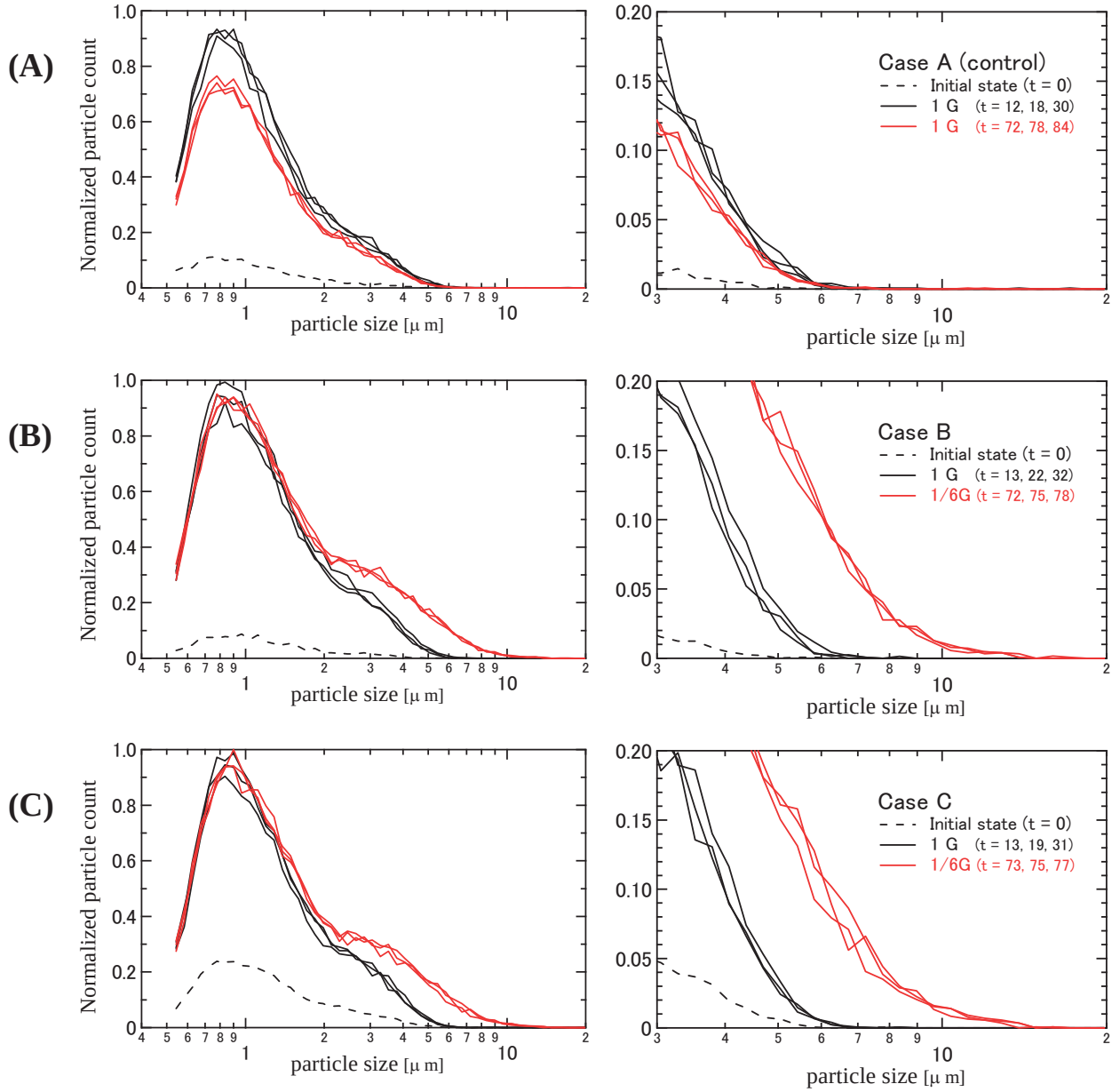


Fig.5 Distribution of the number of particles measured with APS. The axis of ordinates shows the rate of normalized particle count. The axis of abscissas shows the measured particle size $D_p$[μm]. Although the distribution of particle count was measured every second, only 3 points are indicated in the diagrams for each state of gravity. They are indicated by solid lines in black (1G) and in red (1/6G). Each state of gravity in (A)-(C) corresponds respectively to (A)-(C) in Fig.5. Each dotted line shows the distribution of simulant concentration before the start of blowing up and it denotes SPM remaining in the chamber. For horizontal flight (state of 1G) in case A, distribution of particle count classified for particle sizes does not change with time. In cases B and C (state of 1/6G), however, there is an increase in the number of particles under the condition of particle size $D_p$ greater than 1.8 μm. This fact suggests that the duration of particle floating in the state of 1/6G is apparently longer than in the state of 1G.

yellow bar. The time corresponding to typical distribution of data shown in Fig. 5 is indicated by black (1G) and red (1/6G) bars, respectively.

***Results during Horizontal Flight (1G)***

Fig.5 (A) shows the distribution of particles classified by respective particle size as observed during horizontal flight (case A). The right column is an enlarged diagram of the left column, focussing on the vicinity of the cutoff value. The rate of particle count on the axis of ordinates denotes the maximum number, and it is normalized. The cutoff value was calculated with the use of 22 blocks of continuous data obtained from 60 seconds to 82 seconds after the start of blowing up so that it can correspond to the moment when the state of 1/6G is created as a result of parabolic flight.

The results of measurements indicate that the distribution of particles classified by particle size shows changes in concentration with time, but no variations are perceived in the trends of distribution. The mean cutoff value of the Ave.Exp.CVs was calculated to be 5.87 ± 0.22 μm. The results are shown in Table 2.

***Results during Parabolic Flight (1/6G)***

The distribution of particles classified by particle size in case B and case C is shown in Fig. 5 (B) and (C), respectively. The cutoff value was calculated with the use of continuous data collected for 5 to 7 seconds after the creation of the 1/6G state.

Measurements showed the Ave.Exp.CVs of case B to be 13.24 ± 0.53 μm and the Ave.Exp.CVs of case C to be 13.42 ± 0.73 μm. The results are shown in Table 2.

During horizontal flight (case A, state of 1G), the distribution of particles classified by particle size does not change with time. In cases B and C (state of 1/6G), however, an increase is perceived in the number of particles when the particle size is greater than 1.8 μm. This suggests that the duration of particle suspension is extended in the case of 1/6G as compared with 1G.

Table 2. List of cutoff values and results of measurement.

| | 1G | 1/6G | Case |
|---|---|---|---|
| cutoff values | 5.87 ± 0.22 μm | | A |
| | 6.11 ± 0.26 | *3 13.24 ± 0.53 | B |
| | 5.97 ± 0.24 | *4 13.42± 0.73 | C |
| *1 Ave.Exp.CVs | 6.01 | 13.33 | |
| *2 Est.CVs | | 14.73 *5 (9.5%) | |

*1 averaged experimental cutoff values.
*2 theoretically estimated cutoff values. These results were obtained by Stokes' law, on which the cutoff value at 1G (6.01 μm) was based.
*3 We used 5 data to estimate the cutoff values.
*4 We used 7 data to estimate the cutoff values.

## 5. Discussion

As shown in Fig. 5, there was a great increase in the cutoff value in the state of 1/6G compared with the case of 1G. This fact specifies that the SPM in the air was influenced by the gravity. The following section deals with the measurement of the settling speed of the SPM with the use of variations in the cutoff value in order to examine the retention time of lunar regolith on the lunar surface and how the regolith is influenced by gravity.

***Application of Stokes' Law***

By using Stokes' law, the settling speed $v_y$ of particle matter in the air or liquid phase is given by the following equation [24]:

$$v_y = \frac{G\, D_p^2 \left(\rho_p - \rho_{air}\right)}{18\,\mu} \qquad (1)$$

where G, $D_p$, and μ are gravitational acceleration [m/s$^2$], particle size [m], and coefficient of viscosity [Pa·s], respectively. $\rho_p$ and $\rho_{air}$ are the density [kg/m$^3$] of particles and air. Stokes' law is established on the assumption that particles are spherical. Therefore, the settling speed of an actual particle sometimes does not match Stokes' law. Generally, Stokes' law matches well when the Reynolds number ($Re = \rho_{air}\, v_y D_p / \mu$) is small. In this study, the *Re* is became small, since the particle size is too small. On the other hand, if the particle size is extremely small, there will then be an effect of thermal fluctuation caused by Brownian motion, which will result in no conformance to Stokes' law. Thus, Stokes' law is governed by an application range in terms of particle size.

As regards the upper limit of particle size, it is well known that the *Re* number applicable to Stokes' law is $Re < 0.25$ [16]. Therefore, the maximum particle size applicable to Stokes' law, $D_{max}$, is required to satisfy the

following pair conditions:

$$Re = \frac{\rho_{air}\, v\, D_{max}}{\mu} = \frac{G\ D_{max}^3\ \rho_{air}\left(\rho_p - \rho_{air}\right)}{18\,\mu^2} < 0.25$$

$$D_{max} < \left(\frac{4.5\,\mu^2}{G\,\rho_{air}\left(\rho_p - \rho_{air}\right)}\right)^{\frac{1}{3}} \qquad (2)$$

In the case of air at 25°C, air density $\rho_{air}$ and coefficient of viscosity $\mu$ are 1.14 kg/m$^3$ and $1.82 \times 10^{-5}$ Pa·s, respectively. Since the particle density of of FJS-1 $\rho_p$ is $2.96 \times 10^3$ kg/m$^3$ (see Table 1), $D_{max}$ can be calculated from Eq. (2). The results indicate that $D_{max}$ is 35.6 μm for 1G and 64.7 μm for 1/6G, respectively. Since the particle size of FJS-1 used for this experiment was not larger than 20 μm, it was found that the particle size we used was below the upper limit that is applicable to Stokes' law.

The lower limit of the particle size is specified so that the ratio of displacement $\Delta h_2$ versus displacement caused by gravitational settling should be kept at 0.1 or below [16]. Therefore, the minimum particle size applicable to Stokes' law, $D_{min}$, is expressed by the following equations:

$$\frac{\sqrt{K_2\ t / D_{min}}}{D_{min}^2\ t / K_1} < 0.1$$

$$K_1 = \frac{18\,\mu}{G\left(\rho_p - \rho_{air}\right)}, \quad K_2 = \frac{2\,k\,T}{3\,\pi\,\mu} \qquad (3)$$

Here, $k$ is the Boltzmann's constant $1.38 \times 10^{-23}$ kgm$^2$/(s$^2$K) and $t$ is the measuring time [s]. As a result, the following relationship is introduced:

$$D_{min} > \left(\frac{100\ K_1^{\,2} K_2}{t}\right)^{\frac{1}{5}} \qquad (4)$$

Measuring time $t$ shows the duration when the SPM passes through the blades. The cross-sectional area of the elutriator is 25 cm$^2$ and the flow rate of the suction pump is 5 liters/min. Therefore, average flow rate $V_x$ is 33.2 mm/s. Since the length of parallel blades $L_b$ was 10 mm, the time needed to pass through the blades was 0.30 s. When these figures are applied to Eq. (4), $D_{min}$ is defined as 1.15 μm for 1G and 2.35 μm for 1/6G, respectively. Since the cutoff value used for this experiment stayed around 10 μm, it was always above the lower limit of particle size applicable to Stokes' law.

As described above, the simulant used for this experiment was kept within the applicable range of Stokes' law.

### *Relationship between Particle Size and Cutoff Value*

When a particle passes through the blade distance d$H$ at a constant velocity $v_z$, the time $t$ required for the particle to fall down onto the blade surface is given by $t$ = d$H$ / $v_z$. A particle can pass through the elutriator, provided that the mean velocity of the particle is $V_x$, the blade length is $L_b$, and the condition of $t > L_b / V_x$ is satisfied. Since $L_b / V_x$ is a constant then, the following relationship is introduced when Eq. (1) is deformed:

$$1\,G\,D_{1G}^2 = \frac{1}{6}\,G\left(D_{1/6G}\right)^2 \qquad (5)$$

$D_{1G}$ and $D_{1/6G}$ are the particle sizes for 1G and 1/6G, respectively. They are also regarded as the maximum particle sizes that can pass through the elutriator. In other words, this implies that the cutoff value in the state of 1/6G increases to $\sqrt{6}$ times that of 1G.

Using the relationship mentioned above, we estimated the cutoff value in the 1/6G state using the cutoff value of Ave.Exp.CVs for 1G. When 6.01 μm (see Table 2) was given as the cutoff value for 1G, the estimated cutoff value Est.CVs was calculated to be 14.73 μm. We made a comparison of Est.CVs with the experimental results of the 1/6G state by the parabolic flight and found that the empirical figures were smaller than the estimated figures by 9.5%.

Let us consider why the empirical results were lower than the estimated ones. According to Stokes' law, we can assume that 20% of the particles larger than 10 μm will fall down to the chamber bottom before the 1/6G environment is created (i.e. 65 seconds after the start of blowing up). Around the time when the state of 1/6G is finished (i.e. 90 seconds after the blowing up), the initial particle concentration is assumed to go down almost to half the amount. If the effect of the presence of a 30-second hypergravity condition is taken into account, we can suppose that the decrease in the actual number of large particles exceeds the estimated value.

For the aforementioned reasons, we consider that the SPM retention time in the air phase qualitatively conforms to Stokes' law, even though the gravity is changed.

***SPM Retention Time and Gravity***

Using Stokes' law, we investigated the relationship between SPM retention time and gravity while SPM is floating indoors without any convection. We defined the particle size $x$ of SPM and the distribution $N(x)$ of the number of particles. In this case, the total number of SPM particles shortly after the blowing up ($t = t_0$) is given by the following equation:

$$W(t_0) = \int_0^\infty \rho x^3 N(x)\big|_{t_0} dx \qquad (6)$$

Here, ρ denotes the SPM density [kg/m$^3$] and it is assumed that any particles once having fallen down on the floor wil never be blown back up. When the ceiling height $H$ [m] and the settling speed of SPM ν [m/s] are considered, the number of particles $t_1$ seconds after the blowing up is reduced to $(H - \nu \cdot t_1)/H$ times the initial concentration $N(x)|_{t0}$. Therefore, the number of SPM particles suspended at $t = t_1$ is given by the following equation:

$$W(t_1) = \int_0^\infty \rho x^3 N(x)\big|_{t_1} dx = \int_0^\infty \rho x^3 \frac{H - \nu t_1}{H} N(x)\big|_{t_0} dx \qquad (7)$$

The number of SPM particles falling down to the ground from time $t_0$ to $t_1$ is determined by the difference between $W(t_0)$ and $W(t_1)$, and is given by the following equation:

$$\Delta W = W(t_0) - W(t_1) = \int_0^\infty \rho x^3 \frac{\nu t_1}{H} N(x)\big|_{t_0} dx \qquad (8)$$

If the settling speed is applied to Stokes' law, Eq. (8) can be converted into the equation below.

$$\Delta W(t)\big|_{1G} = \int_0^\infty \rho x^3 \frac{G(\rho - \rho_{air})x^2}{18\mu} \frac{t}{H} N(x)\big|_{t_0} dx \qquad (9)$$

Similarly, the number of SPM particles falling down to the ground from time $t_0$ to $t_1$ in the state of 1/6G is determined by the following equation:

$$\Delta W(t)\big|_{lunar} = \frac{1}{6}\int_0^\infty \rho x^3 \frac{G(\rho - \rho_{air})x^2}{18\mu} \frac{t}{H} N(x)\big|_{t_0} dx \qquad (10)$$

When Eq. (9) is compared with Eq. (10), the ratio of the number of SPM particles falling down to the ground is found to be 6. This fact implies that the quantity of SPM staying in the air increases in proportion to the inverse number of gravity. That is, when comparison is made at the same time point, the exposure risk on the Earth is as much high as 6 times greater that on the the surface of the moon.

***Time-Serial Variations in SPM Size and Gravity***

SPM retention time changes with particle size. Large SPM falls down fast, and the rate of minute SPM goes on increasing with time. Therefore, we examined the time-serial variations in SPM size after blowing up by numerical calculation, assuming that the initial condition of particle distribution $N(x)$ was given to Gaussian distribution for the spectrum. We assumed that the mean value of the size of SPM2.5 was 2.5 μm, and the variance $\sigma^2$ was given as 0.3 μm$^2$, based on the results in Fig. 5. The indoor height $H$ was varied from 1 m to 2 m, respectively. Air density $\rho_{air}$, lunar dust density ρ, gravitational acceleration, and coefficient of viscosity for air (at 25°C, 1 atm) were assumed to be 1.184 kg/m$^3$, 2.96 × 10$^3$ kg/m$^3$, 9.81 m/s$^2$, and 1.82 × 10$^{-5}$ Pa·s, respectively [25].

Fig. 6 shows the results of numerical calculation indicating the time-serial variation in the distribution of particle count at 5 minutes, 30 minutes, 1 hour, 3 hours, 6 hours, and 10 hours shortly after the start of blowing up ($t = 0$) while particles of different sizes were still floating inside the room. Under the conditions of $H$ = 1 m and 1G, SPM of 1.7 μm or less stays in the air for more than an hour (red solid line in Fig. 6). At that time, the number of particles sharply decreases from the initial state. Under the conditions of $H$ = 1m and 1/6G, particles of 1.7 μm or less still remain in the air even after the lapse of one hour. The number of overall particles is about half the total amount.

When $H$ = 2 m, SPM remains for a longer time than when $H$ = 1 m. Under the condition of 1/6G, in particular, changes in the number are small compared with the number in the initial state. In particular, SPM of 2 μm or less stays in the air for more than 10 hours.

Next we calculated the 1-meter falling time $FT_{1m}$ of SPM with different particle sizes $D_p$, and the falling velocity $V_e$. $D_p$ was varied to 0.1, 1.0, 2.5, 5.0, 10, and 20 μm, respectively. Table 3 shows the results of computation with the use of Stokes' law. The physical properties used for this computation are the same as the values used in the calculations of Fig. 6.

The floating time of the particles extends longer in a room with a high ceiling, and fine particles can stay suspended in the air even on the earth surface just like their behavior on the lunar surface. This suggests that exposure risk to lunar regolith is associated with not only gravity and particle size but also with ceiling height. For example, the $FT_{1m}$ of SPM with a particle size of 1.0 μm or less is more than 10 hours in 1/6G. Even in the case of

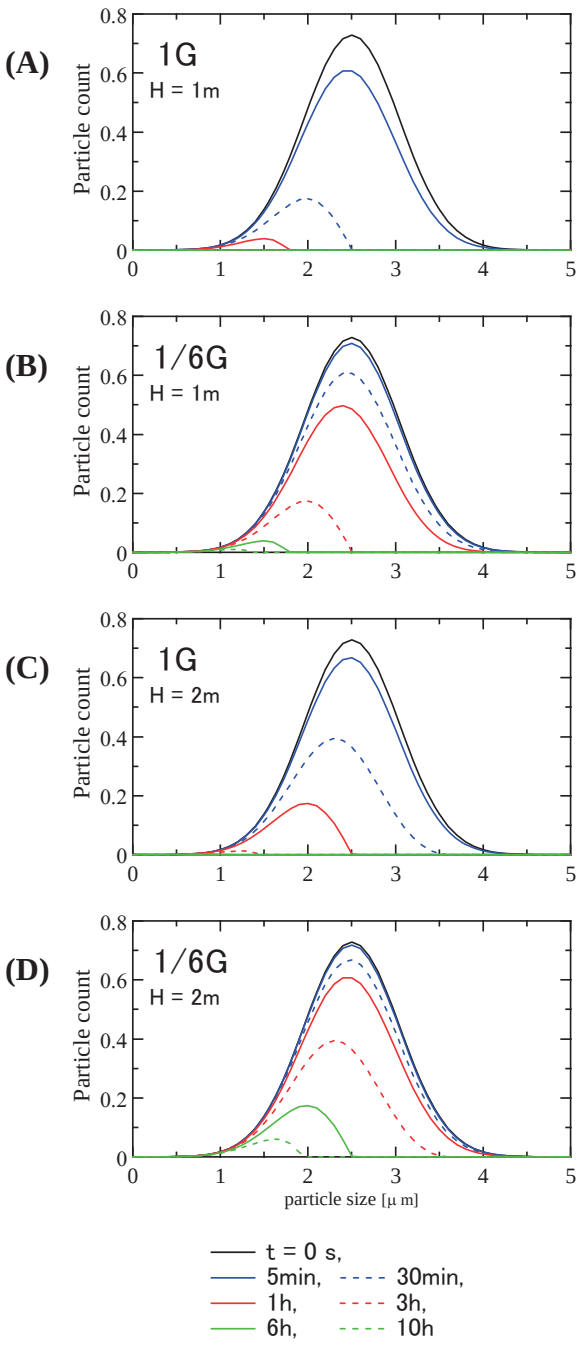


Fig.6 Time-serial variation in distribution of particle count by Stokes' Law ($t$ = 0, 5 min, 30 min, 1 h, 3 h, 6 h, 10 h). $\bar{x}$ = 2.5 μm, $\sigma^2$ = 0.3 μm$^2$, ρ = 2960 kg/m$^3$, $\rho_{air}$ = 1.184 kg/m$^3$, μ = 1.82×10$^{-5}$ Pa·s. (A) Ceiling height $H$ = 1 m, gravity 1G, (B) $H$ = 1 m, 1/6G, (C) $H$ = 2 m, 1G, (D) $H$ =2 m, 1/6G.

Table 3. Estimated falling velocity of SPM classified by particulate size and 1-meter falling time.

| $D_p$ [μm] | 0.1 | 1.0 | 2.5 | 5.0 | 10 | 20 |
|---|---|---|---|---|---|---|
| *2 $v_e$ [m/s] (1G) | 8.9×10$^{-7}$ | 8.9×10$^{-5}$ | 5.5×10$^{-4}$ | 2.2×10$^{-3}$ | 8.9×10$^{-3}$ | 3.5×10$^{-2}$ |
| *2 $v_e$ [m/s] (1/6G) | 1.5×10$^{-7}$ | 1.5×10$^{-5}$ | 9.2×10$^{-5}$ | 3.7×10$^{-4}$ | 1.5×10$^{-3}$ | 5.9×10$^{-3}$ |
| *3 $FT_{1m}$ (1G) | 13 d 1 h | 3 h 8 min | 30 min 1 s | 7 min 31 s | 1 min 53 s | 28 s |
| *3 $FT_{1m}$ (1/6G) | 78 d 9 h | 18 h 49 min | 3 h 0 min | 45 min 9 s | 11 min 17 s | 2 min 49 s |

*1 25°C and 1 atmosphere
*2 $v_e$ : estimated settling velocity
*3 $FT_{1m}$ : 1 meter falling time

1G it is more than 3 hours. SPM of 10 μm or more falls down soon, even in the environment of 1/6G. For particles of 20 μm or more, the $FT_{1m}$ is 28 seconds in 1G, but even in the environment of 1/6G it is 2 minutes and 49 seconds. These results indicate that, as far as fine or large particles are concerned, and so long as we surmise that the longer the floating time, the greater the exposure risk to SPM, it is *unnecessary* to pay attention to the effect of actual gravitational differences between the earth and the moon.

On the other hand, in the case of SPM with particle sizes of 2.5 μm to 10 μm, the floating time on the the surface of the moon increases to 6 times that on the earth, and this effect will make workers feel substantial changes. For example, the value of the $FT_{1m}$ of SPM with a particle size of 2.5 μm is 30 minutes in 1G while it increases to 3 hours for 1/6G. In other words, the safety standard of SPM2.5, which is an object of restriction on the earth, will not be applicable on the moon surface because SPM2.5 keeps floating longer in the environment of 1/6G. It would not be an overstatement to say that more rigorous safety standards will be necessary to avoid exposure risk to lunar regolith on the surface of the moon.

## 6. Conclusion

In anticipation of future human beings living on the lunar surface, we have started research on the prevention of exposure to lunar regolith. We think that this is the first such undertaking in the world. We diffused

simulated lunar regolith under the circumstance of 1/6G created by parabolic flight in order to estimate the SPM floating time, based on variations in the cutoff value of the elutriator. As a result, we have clarified for the first time that the settling speed of SPM in the air phase under the condition of gravity on the moon's surface can be expressed qualitatively by Stokes' law.

Based on this knowledge, we have proven that the SPM floating time increases in proportion to the inverse number of gravity and have defined changes in SPM concentration classified for particle sizes by numerical calculation. As a result, we have come to the conclusion that the lower the gravity and the higher the ceiling height in a room, the longer the working time and the more the labor for decontamination will be.

If exposure risk is assumed to increase as the SPM floating time increases, it is unnecessary to take into consideration the effect of gravity where fine particles of sizes not larger than 1.0 μm or large particles of 10 μm or larger are concerned. Particles with sizes of 2.5 μm to 10 μm, however, fall down sooner on the earth, but they can keep floating for a longer time on the lunar surface. Consequently, we think it will be necessary to take new countermeasures against such particle sizes of SPM by establishing stricter safety standards.

**Acknowledgments**: This paper is based on our previous paper written in Japanese [26]. We newly referred some previous papers [10-15, 17, 22, 23] in this paper. This is the first time that the paper is published to the international journal. This project, based on a joint research contract with the Japan Aerospace Exploration Agency (JAXA) and the National Institute of Occupational Safety and Health, Japan (JNIOSH), was promoted with the support of JAXA. The empirical equipment was designed and manufactured by Shibata Scientific Technology Ltd., to whom we are deeply grateful. We have received much valuable advice from many researchers at the University of Occupational & Environmental Health, Japan. Parabolic flight was realized with the cooperation of Diamond Air Services Ltd. (DAS). The Japan Space Forum also gave us useful advice and supports. We would like to express our deepest gratitude to these people concerned.

## Appendix

In order to investigate the effect of elutriator inclination on the cutoff value, blow-up experiments were carried out by tiling the elutriator on the ground (G1). The direction of inclination corresponded to the coordinate system ($G_x$, $G_y$, $G_z$) shown in Fig.1. During this research, we examined two cases when the elutriator was tilted by ±10° in the direction of Axis $G_y$, and when it was tilted by 10°, 45°, and 90° in the direction of Axis $G_x$.

The results of the experiments on the ground indicate that there is almost no influence on the cutoff value, provided that the tilting angle is kept within ±10° (Fig.7(A)~(C)). When the tilting angle is 45° or more, there are apparently some changes, as shown in Fig.7 (D) and (E), impying that, during parabolic flight, the effect of the inclination of aircraft is small.

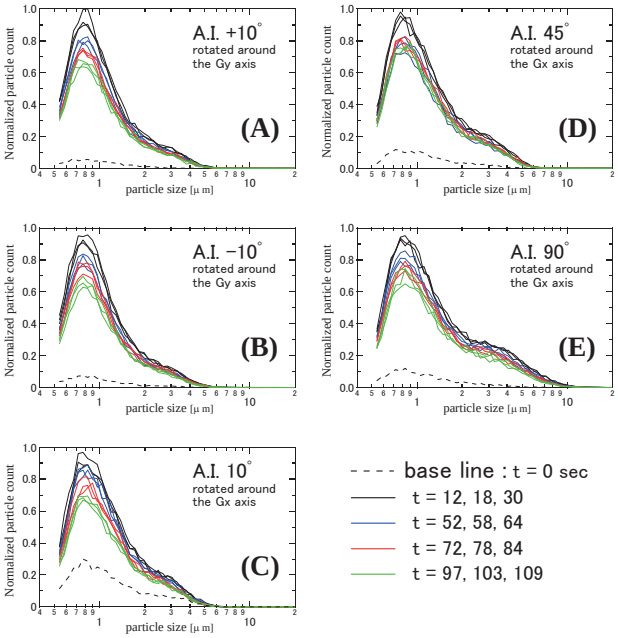


Fig.7 Effect of elutriator inclination. Tilting angle (A.I) is: (A) Tilted by +10° against Axis $G_y$, (B) Tilted by -10° against Axis $G_y$, (C) Tilted by 10° against Axis $G_x$, (D) Tilted by 45° against Axis $G_x$, (E) Tilted by 90° against Axis $G_x$. So long as the tilting angle is kept within ±10°, almost no influence is perceived on the cutoff value.

## References


1) U.S. Congress, Office of Technology Assessment. Exploring the Moon and Mars: Choices for the Nation 1991. Washington, DC: U.S. Government Printing Office.
2) Kanamori H. Properties of lunar soil simulant manufactured in Japan. Proceeding of the 6th International Conference and Exposition on Engineering, Construction, and Operations in Space; 1998.
3) Park J, Liu Y, Kihm KD, Taylor LA. Characterization of lunar dust for toxicological studies. I: particle size distribution, Journal of Aerospace Engineering 2008; 21: 266-271.
4) Liu Y, Park J, Schnare D, Hill E, Taylor LA. Characterization of lunar dust for toxicological studies. II: texture and shape characteristics, Journal of Aerospace Engineering 2008; 21: 272-279.
5) Wallace WT, Taylor LA, Liu Y, Cooper BL, McKay DS, Chen B, Jeevarajan AS. Lunar dust and lunar simulant activation and monitoring. Meteoritics and Planetary Science 2009; 44: 961-970.
6) Heinemann M. Shuttle contamination modeling. Space Physics Division, Air Force Geophysics Laboratory in Hanscom AFB, MA.;1985.
7) Pierson DL. Microbial contamination of spacecraft, Gravitational and Space Biology Bulletin 2001; 14.
8) Song B, Leff LG. Identification and characterization of bacterial isolates from the Mir space station. Microbiological Research 2005; 160: 111-117.
9) Bernold, L. Experimental studies on mechanics of lunar excavation, Journal of Aerospace Engineering 1991; Vol. 4: 9-22.
10) Miki, T., Aoki, S., Morimoto, Y., Tanaka, K., Shimada, K., Mukai., C. Human risk assessment for in-situ lunar dust measurement, Annual Meeting of the Lunar Exploration Analysis Group, Nov. 16–19, Houston, Texas, p 41, 2009.
11) Miki, T., Morimoto, Y., Higashi, T., Tanaka, K., Mukai., C. Lunar dust problem on human body (*in Japanese*), International Journal of Microgravity Science and Application 2009; 26: 303-308.
12) Darquenne, C., Paiva, M., West, J. B., Prisk, G. K. Effect of microgravity and hypergravity on deposition of 0.5- to 3-μm diameter aerosol in the human lung, Journal of Applied Physiology 1997; 83: 2029-2036.
13) Darquenne, C., West, J. B., Prisk, G. K. Deposition and dispersion of 1-μm aerosol boluses in the human lung: effect of micro- and hypergravity: Journal of Applied Physiology 1998; 85: 1252-1259.
14) Darquenne, C., West, J. B., Prisk, G. K. Dispersion of 0.5- to 2-μm aerosol in μG and hypergravity as a probe of convective inhomogeneity in the lung: Journal of Applied Physiology 1999; 86: 1402-1409.
15) Darquenne, C., Paiva, M., Prisk, G. K. Effect of gravity on aerosol dispersion and deposition in the human lung after periods of breath holding, Journal of Applied Physiology 2000; 89: 1787-1792.
16) Japan Industrial Standard, Particle size measurement with gravity sedimentation in a liquid phase, 2002; JIS Z8820-1.
17) Kamiya H, Research and development on international standard measurement and analysis method for emission behavior of suspended particular matter from stationary sources (*in Japanese*). Earozoru Kenkyu (Journal of Aerosol Research) 2007; 22: 296-301.
18) Onishi, Y., Fujita, O., Agata, K., Takeuchi, H., Nakamura, Y., Ito, H., Kikuchi, M., Observation of flame spreading over electric wire under reduced gravity condition given by parabolic flight and drop tower experiments, Trans. JSASS Space Tech. Japan, 2010; 8: 19-24.
19) Maki S, Ataka M. Suppression and promotion of convection in water by use of radial components of the magnetization force. Journal of Applied Physics 2004; 96: 1696-1703.
20) Maki S, Ataka M. Three-dimensional computation of convection of water at the center of a superconducting magnet. M. Physics of Fluids 2005; 17: 087107-1 – 087107-7.
21) Japan Industrial Standard, Test method for minimum explosible concentration of combustible dusts, 2002; JIS-Z8818.
22) Maki, S., Han, J., Aoki, S., Okuno, M., Tanimoto, Y., Udagawa, C., Morimoto, S., Fujiwara, M., Fujiwara, Y. and Inoue, K., Magnetism of Simulated Lunar Regolith of FJS-1, International Journal of Biomedical Soft Computing and Human Sciences 2014; 19: 35-38.
23) Hapke, B., Cassidy, W. and Wells, E. Effects of vapor-phase deposition processes on the optical, chemical, and magnetic properties of the lunar regolith, The Moon 1975; 13: 339-353.
24) Jackson ML, Barak P. Soil Chemical Analysis:

Advanced Course Revision of 2nd edition, Wisconsin: Parallel Press, University of Wisconsin-Madison Libraries; 1985. chapter 3.1, p110.
25) Holman JP. Heat Transfer: (7th edition in SI Units). London: McGraw-Hill Book Co., 1992. p. 663.
26) Maki, S., Tanaka, K., Tsuchiya, H., Aoki, S., Takeoka, H., Miki, T., Honma, Y., Ohshima, H., Yamamoto, M., Morimoto, Y., Ogawa, Y. and Mukai. C. "Research on lunar dust exposure on the moon surface; atmospheric suspension of simulated lunar dust in 1/6 G environment by a parabolic flight (*in Japanese*)," Journal of Biomedical Fuzzy Systems 2013; 15: pp. 7-18.

**Syou MAKI**
He received a Dr. degree of eng. from Kyushu Univ. in 2002. Since 2012, he has been working at Faculty of Pharmacy, Osaka Ohtani Univ. His research interests include magnetic convection, protein crystallizatgion with a magnetic force, and data mining. He is a member of BMFSA.

**Yoshiyuki HONMA**
He was a member of Space Biomedical Research Office, Japan Aerospace Exploration Agency. Dr.(M.D.).

**Hidetoshi TSUCHIYA**
He was a member of Space Biomedical Research Office, Japan Aerospace Exploration Agency.

**Kazunari TANAKA**
He was a member of Space Biomedical Research Office, Japan Aerospace Exploration Agency. Now he is Director General of Tokyo Quarantine Station, Ministry of Health, Labour and Welfare. Dr.(M.D.).

**Shigeru AOKI**
He was a member of Space Biomedical Research Office, Japan Aerospace Exploration Agency. His present affiliation is Institute of Technology, SHIMIZU Corporation.

**Hajime TAKEOKA**
He was a member of Space Biomedical Research Office, Japan Aerospace Exploration Agency. His present affiliation is Department of Science and Applications, Life Science Group, Japan Space Forum.

**Takeo MIKI**
He is a member of Space Biomedical Research Office, Japan Aerospace Exploration Agency. Dr.(M.D.).

**Hiroshi OHSHIMA**
He is a member of Space Biomedical Research Office, Japan Aerospace Exploration Agency. Dr.(M.D.).

**Masafumi YAMAMOTO**
He was a member of Space Biomedical Research Office, Japan Aerospace Exploration Agency. Now he is a Deputy Center Director, Tsukuba Space Center, Japan Aerospace Exploration Agency.

**Yasuo MORIMOTO**
He is a professor of Department of Occupational Pneumology, University of Occupational and Environ -mental Health, Japan. Dr.(M.D.).

**Yasutaka OGAWA**
He is a president of the National Institute of Occupational Safety and Health, Japan (JNIOSH). Dr.(M.D.).

**Chiaki MUKAI**
She is a Director of Center for Applied Space Medicine and Human Research, Japan Aerospace Exploration Agency. Dr.(M.D. and Ph.D.).